PhotoniX

RESEARCH Open Access

Ultrafast dissipative soliton generation in anomalous dispersion achieving high peak power beyond the limitation of cubic nonlinearity

Jinhwa Gene[1], Seung Kwan Kim[2], Sun Do Lim[2*] and Min Yong Jeon[3,4*]

*Correspondence: sdlim@kriss.re.kr; myjeon@cnu.ac.kr

[1] Artificial Intelligence Research Laboratory, Electronics and Telecommunications Research Institute, Daejeon 34129, Republic of Korea
[2] Division of Physical Metrology, Korea Research Institute of Standards and Science, Daejeon 34113, Republic of Korea
[3] Institute of Quantum Systems (IQS), Chungnam National University, Daejeon 34134, Republic of Korea
[4] Department of Physics, College of Natural Sciences, Chungnam National University, Daejeon 34134, Republic of Korea

Abstract

The maximum peak power of ultrafast mode-locked lasers has been limited by cubic nonlinearity, which collapses the mode-locked pulses and consequently leads to noisy operation or satellite pulses. In this paper, we propose a concept to achieve mode-locked pulses with high peak power beyond the limitation of cubic nonlinearity with the help of dissipative resonance between quintic nonlinear phase shifts and anomalous group velocity dispersion. We first conducted a numerical study to investigate the existence of high peak power ultrafast dissipative solitons in a fiber cavity with anomalous group velocity dispersion (U-DSAD) and found four unique characteristics. We then built long cavity ultrafast thulium-doped fiber lasers and verified that the properties of the generated mode-locked pulses match well with the U-DSAD characteristics found in the numerical study. The best-performing laser generated a peak power of 330 kW and a maximum pulse energy of 80 nJ with a pulse duration of 249 fs at a repetition rate of 428 kHz. Such a high peak power exceeds that of any previous mode-locked pulses generated from a single-mode fiber laser without post-treatment. We anticipate that the means to overcome cubic nonlinearity presented in this paper can give insight in various optical fields dealing with nonlinearity to find solutions beyond the inherent limitations.

Introduction

Mode-locked fiber lasers have been favored in various fields where ultrashort pulse durations and high peak powers and intensities are demanded. Ultrashort pulse durations are useful in applications such as range-finding and lidar systems using the time-of-flight method to achieve high resolution and high accuracy [1–4], and high peak powers of mode-locked pulses are advantageous in nonlinear optics, medical surgery, and material processing [5–9]. For these applications, various approaches to enhancing the properties of mode-locked lasers have been researched.

One effort is to increase the peak power of mode-locked pulses by shortening the pulse duration or increasing the pulse energy. Increasing peak power remains a subtle

and sophisticated challenge due to inherent limitations from nonlinear phase shifts in the fiber medium that can break a mode-locked pulse into pieces and drive the lasers to noisy operation [10–13]. Many efforts have been made to reduce the accumulation of nonlinear phase shifts for pulse amplification in laser cavities or post-amplification; examples include applying large mode area fibers or chirped pulse amplification [14–22]. These methods reduce the effective nonlinearity by alleviating the mode-locked pulse intensity through dispersing the pulse field in the time domain or over the transverse area of the fiber medium. However, laser systems applying these approaches are still under the limitation of nonlinearity and are complicated by the need for sophisticated parameter control [23–27].

Another approach to enhance the properties of mode-locked lasers is to optimize the mode-locking operation regimes for applications, such as soliton, dissipative soliton, ultrafast dissipative soliton, similariton, stretched pulse, and dispersion-managed mode-locked lasers, which can be conducted together with the other methods mentioned above [10, 28–31]. Recently, a new mode-locking solution of dissipative resonance has been found in anomalous group velocity dispersion (GVD) [32, 33]. Typically, dissipative solitons can be generated in normal GVD cavities by the help of dissipative resonance between normal GVD and cubic nonlinearity, where both drive the pulse to have positive chirp [29, 30]. However, in the case of dissipative solitons in anomalous GVD (DSAD), dissipative resonance derives from anomalous GVD and quintic nonlinearity, where both drive the pulse to have negative chirp when the quintic nonlinearity is negative. The solution of DSAD was first presented by Chang et al. in 2009 [32] based on the cubic-quintic Ginzburg–Landau equation, after which DSAD was experimentally demonstrated by Liu et al. in 2011 with square-shaped pulses in the time domain, where the pulse duration was extended with constant peak power as the pump power increased [33]. Following this first realization, DSAD has been further studied [34–37], but to date demonstrations of DSAD have only shown dissipative soliton pulses with a square-shape in the time domain. In other words, ultrafast dissipative solitons have yet to be generated in anomalous GVD.

In this paper, we demonstrate a fiber laser exhibiting ultrafast dissipative solitons in a fiber cavity with anomalous group velocity dispersion, or U-DSAD, with a negative quintic nonlinearity, along with the finding that the generation of ultrafast dissipative solitons can realize a high peak power beyond the limitation of cubic nonlinearity. We first investigate and characterize the properties of U-DSAD through a numerical study with Haus's master equation, based on which we propose a principle to generate an ultrafast mode-locked pulse with a high peak power beyond the limitation of cubic nonlinearity. In short, chirps induced by the quintic nonlinearity of the fiber medium compensate the chirps induced by the anomalous dispersion, and this can be exploited to build U-DSAD. Through the numerical study, four unique properties of U-DSAD are found that are quite different from those of typical solitons and dissipative solitons. Based on the numerical study, we then generate U-DSAD with a low repetition rate mode-locked thulium-doped silica fiber (TDF) laser employing the nonlinear polarization rotation (NPR) method. To realize U-DSAD, a few hundred meters long fiber ring cavity is necessary to achieve high total nonlinearity and high total dispersion values with the single-mode fiber used in this work (Thorlabs SM2000). The total length of the fiber cavity is

485 m, and the repetition rate of the mode-locked laser is 427 kHz with a total GVD of −43.7 ps^2 and cubic nonlinearity of 0.22 W^{-1}. The constructed laser is confirmed to exhibit the four unique properties of U-DSAD found in the numerical simulation. The pulse duration and energy of the mode-locked pulse are 249 fs and 80 nJ, respectively. Assuming the pulse shape to be Gaussian in the time domain, the peak power of the pulse is estimated to be 330 kW, a peak power exceeding that of any previous single-mode fiber lasers. We anticipate that the present demonstration of U-DSAD is useful for a wide range of high peak power applications, such as nanomachining, drilling, corneal surgery, and nonlinear optics. Moreover, as this paper presents a method to achieve high peak power beyond the limitation of cubic nonlinearity, the results can give insight not only to research fields focused on mode-locked fiber lasers but also to a variety of optical fields dealing with optical nonlinearity to overcome inherent nonlinearity.

Principles

The self-phase modulation (SPM) of a mode-locked pulse by nonlinear phase shifts is one of the most important factors to stabilize mode-locked lasers and determine the mode-locking regime. Up to now, cubic nonlinearity has attracted the most interest to express mode-locking regimes and to study mode-locking stability. Quintic nonlinearity, on the other hand, has been mostly negligible in high power applications such as pulse explosion or soliton collisions. However, dissipative soliton (DS) solutions have been found in anomalous GVD on account of quintic nonlinearity, and thus quintic nonlinearity is indispensable to study high peak power mode-locked lasers [32, 38, 39].

We can write the refractive index with nonlinear phase shifts induced by cubic and quintic nonlinearity as

$$n = n_0(\omega) + n_2 \cdot |E|^2 + n_4 \cdot |E|^4, \tag{1}$$

where n_0 is the linear refractive index, and n_2, n_4 are the nonlinear refractive indices by cubic and quintic nonlinearity, respectively. Figure 1a shows the amount of nonlinear phase shift with respect to optical intensity when the value of n_4 is negative. At a low intensity level, the amount of nonlinear phase shift linearly increases as the intensity increases. As the intensity further strengthens, at some point, the nonlinear phase shift arising from quintic nonlinearity overwhelms that by cubic nonlinearity, and consequently, the amount of nonlinear phase shift decreases. An increment in the nonlinear phase shift drives the mode-locked pulse to have positive chirp in the time domain, while conversely, a decrement leads to negative chirp. Typically, DS can be generated from dissipative resonance between two positive chirps induced by normal GVD and cubic nonlinearity. In a similar way, we expect that dissipative resonance can also be made at intensities higher than I_C, but in the opposite direction, by two negative chirps derived from anomalous GVD and negative quintic nonlinearity [32–37]. The intensity levels for stable solutions of DS and U-DSAD are marked in Fig. 1a. Figure 1b shows the chirp direction in a typical DS pulse, where the arrows point in the direction of increasing optical field frequency. For example, positive chirp, where the high-frequency optical components are delayed in the time domain, points in the + direction. Chirps induced by normal GVD and by nonlinearity have the same direction and are quite uniform throughout the DS pulse. Correspondingly, Fig. 1c shows the chirp direction in U-DSAD

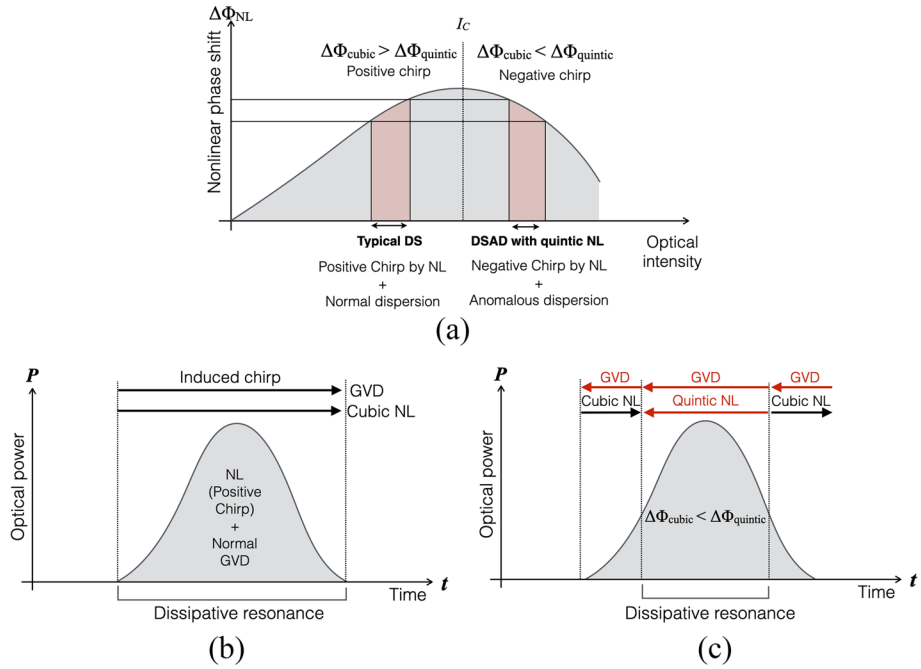

Fig. 1 **a** Nonlinear phase shift with respect to optical intensity. **b** Optical power profile and chirp direction in a typical dissipative soliton pulse with normal GVD and cubic nonlinearity. **c** Optical power profile and chirp direction in an ultrafast dissipative soliton pulse with anomalous GVD and quintic nonlinearity

driven by anomalous GVD and nonlinearity. While the amount and direction of chirp induced by GVD is almost uniform throughout the pulse, the direction of chirp induced by nonlinearity is a function of optical intensity for U-DSAD. The pulse center, where the intensity is higher than I_C, has negative chirp, as GVD does. Otherwise, the trailing and leading edges of the pulse, having intensities lower than I_C, have an opposite chirp direction than that by cubic nonlinearity. We anticipate that this nonuniform chirp structure of U-DSAD creates unique characteristics, which we explore via numerical calculations in the next section.

Numerical calculation

To find stable solutions of U-DSAD, we conducted numerical calculations of Haus's master equation with cubic-quintic nonlinearity. Haus's master equation in fundamental form with cubic-quintic nonlinearity is written as follows [38–42]:

$$E_{n+1}(t) = e^{-l_0} \cdot e^{-i\cdot\left(\gamma\cdot|E|^2+\nu\cdot|E|^4\right)\cdot L} \cdot e^{-i\cdot\beta_2(\omega)\cdot L} \cdot e^{-q(t)} \cdot e^{G(\omega,t)} \cdot E_n(t - T_R) \tag{2}$$

$$G(\omega,t) = g(\omega_0,t)\cdot\left(1 + i\frac{\omega-\omega_0}{\omega_{bw}}\right)^{-1} \tag{3}$$

$$g(\omega_0,t) = \frac{g_0(\omega_0)}{1+|E(t)|^2/P_{sat,g}}, \tag{4}$$

$$q(t) = \frac{q_0}{1 + |E(t)|^2 / P_{sat,q}} \tag{5}$$

where E_{n+1}, E_n denote the electric field that has completed n + 1 and n round trips in the laser cavity, respectively, l_0 is the total loss of the cavity including the fibers and components in the cavity, γ, ν are factors of cubic and quintic nonlinearity, respectively, L is the total length of the fiber cavity, $\beta_2(\omega)$ is the GVD parameter, $q(t)$ is the saturable absorption, $G(\omega,t)$ is the gain that depends on optical frequency and time, $g_0(\omega_0)$ is the small signal gain at the maximum point in the optical frequency domain, q_0 is the small signal absorption of saturable absorption, and $P_{\mathrm{sat,g}}$ and $P_{\mathrm{sat,q}}$ are the saturation power of the gain and saturable absorption, respectively. Cubic and quintic nonlinearity are expressed as $\gamma = n_2/k_0$ and $\nu = n_4/k_0$, respectively. The spectral gain shape is assumed to be Gaussian, as shown in Eq. (3), with a spectral gain bandwidth of ω_{bw}. As Haus's master equation is an integrated form of the nonlinear Schrödinger equation (or Ginzburg–Landau equation) for a round trip and the total absolute values per round trip of GVD, nonlinearity, and loss are too large to merge them into a single value, these have to be calculated with a split-step Fourier method.

For the calculations, we set the values of the mode-locked laser as shown in Table 1. In this condition, we found a soliton mode-locking operation with the help of anomalous GVD and cubic nonlinearity. Figure 2a shows stable mode-locked operation with soliton pulses in the time domain when $P_{sat,g} = 6\ mW$, $\gamma = 2 \times 10^{-3}\mathrm{W}^{-1}\mathrm{m}^{-1}$, $\nu = 0$. The optical spectrum of soliton operation with a Kelly sideband and hyperbolic secant spectral shape is shown in Fig. 2d.

Since our interest is to discover the solution of U-DSAD at higher power levels, we checked the intensity profile in the time domain with increasing $P_{sat,g}$. When $P_{sat,g}$ is 63 mW, the intensity profile becomes noisy without quintic nonlinearity, as shown in Fig. 2b and e. With some amount of quintic nonlinearity, $\nu = -5.55 \times 10^{-7}\mathrm{W}^{-2}/\mathrm{m}$, however, we found that a solution of stable mode-locking indeed exists, as shown in Fig. 2c and f. Another noteworthy property is that the optical spectrum of a mode-locked pulse with quintic nonlinearity exhibits a trapezoidal shape with a flat top. A trapezoidal optical spectrum is not typical of mode-locked lasers, but some dissipative solitons have been observed to exhibit such a spectrum shape when the total nonlinearity and GVD of the cavity are high enough [43, 44]. The stable mode-locked pulses in Fig. 2c and f seem

Table 1 Definition of the parameters and their values used in the numerical calculation

Parameter	Definition	Value
L	Total length of cavity	30 m
γ	Cubic nonlinearity (SPM)	$2 \times 10^{-3}\mathrm{W/m}$
ν	Quintic nonlinearity (SPM)	Variable
q_0	Modulation depth of saturable absorption	5.7 dB
$g_0(\omega_0)$	Peak small signal gain at ω_0	10 dB
ω_{bw}	Spectral gain bandwidth	100 nm
l_0	Total loss of the cavity	4 dB
$\beta_2(\omega)$	Group velocity dispersion (GVD)	$-8 \times 10^{-2}\mathrm{ps}^2/\mathrm{m}$
n_0	Linear refractive index	1.45

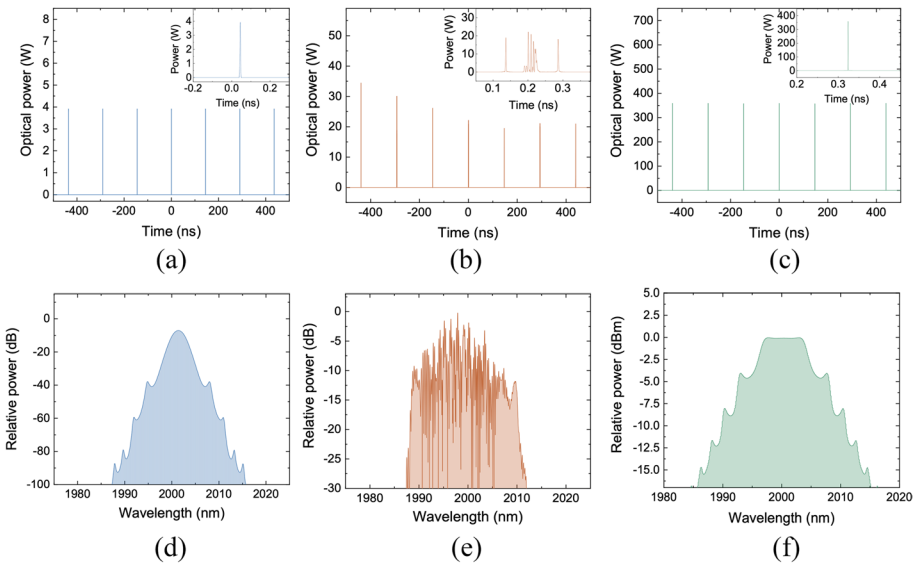

Fig. 2 Optical power profile in the time domain of a mode-locked laser with anomalous GVD (soliton) when (**a**) $P_{sat,g} = 6\ m\mathrm{W}, \gamma = 2 \times 10^{-3}\mathrm{W}^{-1}\mathrm{m}^{-1}, \nu = 0$, **b** $P_{sat,g} = 63\ m\mathrm{W}, \gamma = 2 \times 10^{-3}\mathrm{W}^{-1}\mathrm{m}^{-1}, \nu = 0$, and **c** $P_{sat,g} = 63\ m\mathrm{W}, \gamma = 2 \times 10^{-3}\mathrm{W}^{-1}\mathrm{m}^{-1}, \nu = -5.55 \times 10^{-7}\mathrm{W}^{-2}/\mathrm{m}$. Optical spectrum when (**d**) $P_{sat,g} = 6\ m\mathrm{W}, \gamma = 2 \times 10^{-3}\mathrm{W}^{-1}\mathrm{m}^{-1}, \nu = 0$, **e** $P_{sat,g} = 63\ m\mathrm{W}, \gamma = 2 \times 10^{-3}\mathrm{W}^{-1}\mathrm{m}^{-1}, \nu = 0$, and **f** $P_{sat,g} = 63\ m\mathrm{W}, \gamma = 2 \times 10^{-3}\mathrm{W}^{-1}\mathrm{m}^{-1}, \nu = -5.55 \times 10^{-7}\mathrm{W}^{-2}/\mathrm{m}$. The insets in (**a**–**c**) show a magnified view of a pulse in the time domain

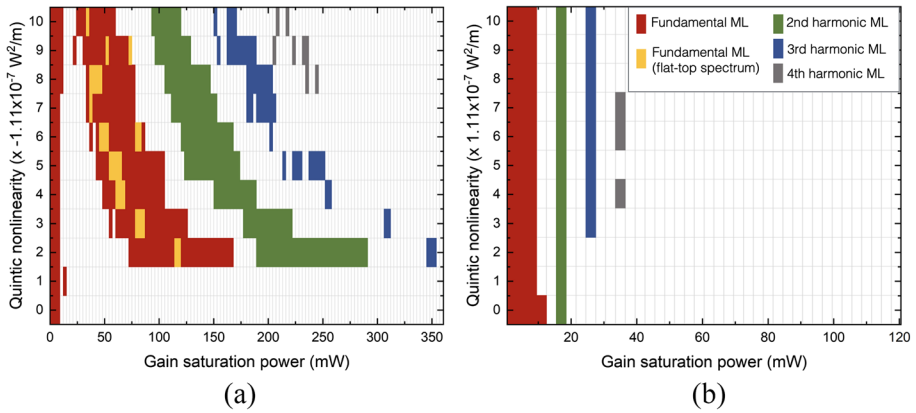

Fig. 3 **a** Parameter ranges for a stable mode-locking (ML) solution with respect to gain saturation power ($P_{sat,g}$) and negative quintic nonlinearity (ν). Each colored area shows the condition for stable mode-locking. **b** Parameter ranges for stable mode-locking with positive quintic nonlinearity

to be built by dissipative resonance between anomalous GVD and quintic nonlinearity. Based on the results, we presume that quintic nonlinearity is an important factor for the solution of stable mode-locking with high peak power and high pulse energy.

To clarify that dissipative resonance is one of the key factors for mode-locking solutions at high peak power, we conducted numerical calculations of Haus's master equation over a broad range of parameter values. Figure 3a shows the parameter ranges for stable mode-locking solutions with respect to gain saturation power ($P_{sat,g}$) and quintic nonlinearity (ν) from numerical calculations. Each colored point in the figure indicates a condition where stable mode-locking is observed: red indicates fundamental

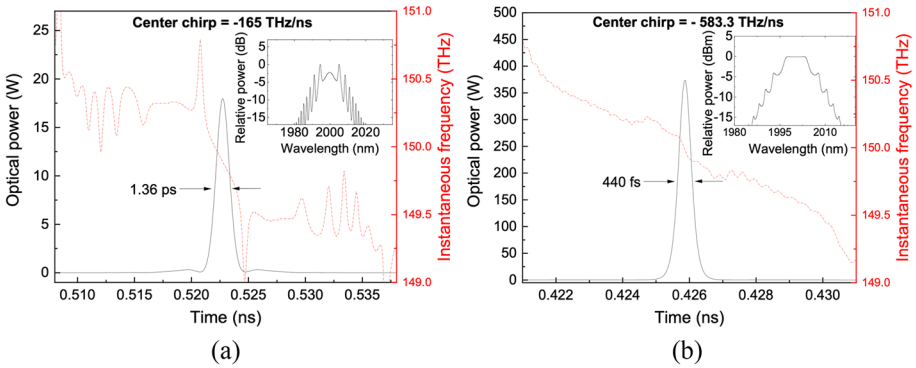

Fig. 4 **a** Power profile of a soliton pulse in the time domain and its instantaneous frequency with $\nu = 0, P_{sat,g} = 9\text{mW}$. **b** Power profile of U-DSAD in the time domain and its instantaneous frequency with $\nu = -5.55 \times 10^{-7}\text{W}^{-2}/\text{m}, P_{sat,g} = 63\text{mW}$

mode-locking, yellow indicates fundamental mode-locking with a flat-top optical spectrum as in Fig. 2f, and green, blue, and gray indicate 2nd, 3rd, and 4th harmonic mode-locking, respectively. The results distinctly show different solution regimes in terms of gain saturation power. Under 10 mW, typical soliton solutions are found with hyperbolic secant-shaped pulses, and the solution regime seems to be independent of the value of quintic nonlinearity. It is natural that soliton solutions are constructed by cubic nonlinearity and anomalous dispersion when the effect of quintic nonlinearity is low. But with increasing gain saturation power, other solutions are found that exhibit atypical properties of mode-locking. When $\nu = -2.22 \times 10^{-7}\text{W}^{-2}/\text{m}$, solutions are found from 75 to 168 mW, where no stable mode-locking solution has previously been found with cubic nonlinearity alone. Unlike typical soliton solutions at low $P_{sat,g}$, the solutions above a $P_{sat,g}$ of 25 mW depend on the amount of quintic nonlinearity, where the value of $P_{sat,g}$ for a stable solution regime decreases as that of quintic nonlinearity increases. Another remarkable point is that some of these solutions exhibit a flat-top optical spectrum. The parameter values of fundamental mode-locking solutions with a flat-top spectrum are marked on the parameter map in yellow in Fig. 3a.

To look inside these mode-locking solutions, the instantaneous frequency of a mode-locked pulse at low $P_{sat,g}$ is compared to one at high $P_{sat,g}$. Figure 4a shows the instantaneous frequency of a pulse with typical soliton mode-locking. The pulse chirp, which is defined as the slope of the instantaneous frequency in the time domain, is the lowest at the center of the pulse due to counteractions between cubic nonlinearity and anomalous GVD. The leading and trailing edges of a soliton pulse have stronger chirp in the direction of GVD due to decrements in the chirp induced by cubic nonlinearity at low power. One solution at high $P_{sat,g}$ shows different properties in terms of chirp, as shown in Fig. 4b. Here, the pulse center has the strongest chirp, while the leading and trailing edges have lower chirp. The strongest chirp at the center of the pulse is −583.3 THz/ns. At the pulse center, strong chirp can be made by the coaction of quintic nonlinearity and anomalous GVD that induces chirp in the same direction. At each edge with low power, cubic nonlinearity is dominant, and consequently, the amount of chirp decreases. This characteristic matches well with our expectation about U-DSAD shown in Fig. 1c.

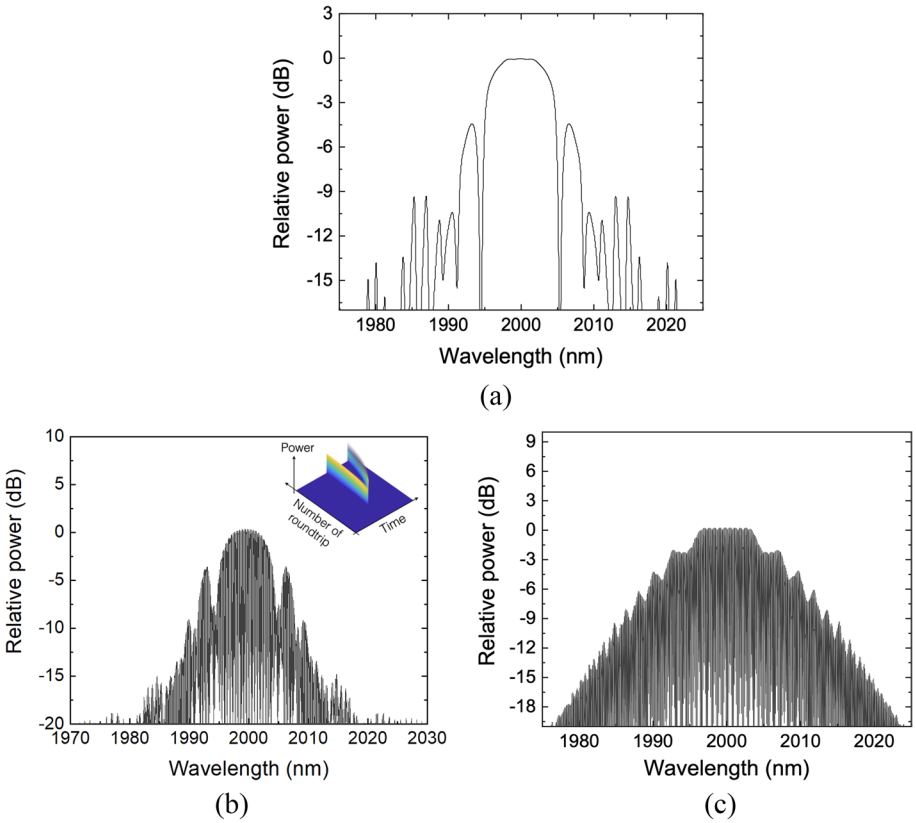

Fig. 5 **a** Optical spectrum of fundamental mode-locking with $\nu = -5.55 \times 10^{-7} \mathrm{W}^{-2}/\mathrm{m}, P_{sat,g} = 78$ mW. **b** Optical spectra of 2nd harmonic mode-locking with $\nu = -5.55 \times 10^{-7} \mathrm{W}^{-2}/\mathrm{m}, P_{sat,g} = 141$ mW, and **c** that with $P_{sat,g} = 165$ mW. The inset in **b** shows the optical power profile in the laser cavity evolving to 2nd harmonic mode-locking

Based on these properties, we can say that the solutions found at higher $P_{sat,g}$ are U-DSAD built by dissipative resonance between anomalous dispersion and quintic nonlinearity. Due to the fact that the solutions are built by nonlinearity, optical spectra in the solution region have various shapes with respect to $P_{sat,g}$. Figure 5a shows an optical spectrum with a shape totally different from that in Fig. 2f. Another atypical characteristic of the U-DSAD solutions is the feasibility of harmonic mode-locking with any shape of the optical spectra. Generally, harmonic mode-locking with a passive mode-locker can be realized in soliton operation with a hyperbolic secant optical spectrum; harmonic mode-locking is not typical for DSs. Some studies show that harmonic mode-locking of DSs in normal dispersion can be made by strong spectral filtering to saturate the pulse energy. However, in our calculations, no spectral filtering effect is made in the cavity. Harmonic mode-locking of U-DSAD is made naturally by the coaction of nonlinear phase shifts and GVD with various optical spectra shapes, as shown in Fig. 5b and c. The reason why the spectra in Fig. 5b and c look noisy is that the longitudinal modes corresponding to mode orders having odd numbers are suppressed for 2nd harmonic mode-locking.

Based on the numerical study, we found mode-locking solutions of U-DSAD and characterize four unique properties as below.

I. The pulse energy of U-DSAD is much higher than typical soliton pulse energy. At most, it is about 18 times higher in the current work.
II. Some of the solutions exhibit a flat-top spectrum, which has not previously been found in soliton solutions with anomalous dispersion.
III. The optical spectra of U-DSAD vary with respect to $P_{sat,g}$.
IV. Harmonic mode-locking with dissipative resonance without spectral filtering is feasible.

We believe that these characteristics distinguish DS and U-DSAD and can provide evidence of U-DSAD generation in fiber lasers.

Experiments

Based on the numerical calculations, both anomalous dispersion and high nonlinearity with sufficient quintic nonlinear effects are necessary to realize U-DSAD in fiber lasers. Most experimental cases of DSAD have been demonstrated with TDF lasers in many previous studies [32–37]. This is assumed to be because silica fiber has a negative value of quintic nonlinearity and properly matches the anomalous dispersion for dissipative resonance at a wavelength of 2 μm with the average power of typical single-mode fiber lasers (under few hundreds of mW). Accordingly, we presume that low repetition rate mode-locked TDF lasers are the best choice for U-DSAD [32, 33, 40, 44]. A laser with a low repetition rate can achieve a high pulse energy by elongating the fiber cavity to a few hundred meters [45–47]. Furthermore, the amount of dissipative resonance is proportional to the length of the fiber cavity. Numerous factors determine the solution of mode-locked pulses, including spectral shape, recovery dynamics of gain and saturable absorption, amount of gain and loss at each component, etc. To maximize dissipative resonance, a long fiber cavity is essential.

Following this idea, we built low repetition rate mode-locked TDF lasers for U-DSAD. The host material of the fiber is silica. Figure 6 shows a schematic of the low repetition rate mode-locked TDF laser for U-DSAD. For effective allocation of gain into the long fiber cavity, two TDF amplifiers were made. Each TDF amplifier is made of 4 m long TDF (Nufern SM-TDF10/130) and pumped by a laser diode (LD) at a wavelength of 793 nm through a beam combiner (BC). The rest of the passive fiber is single-mode silica fiber (Thorlabs SM2000). Mode-locking of the laser is realized by the NPR technique since the long fiber cavity has a quite large amount of loss by silica glass absorption at 2 μm wavelength, and thus strong saturable absorption is essential [40–42].

We tested four different lengths of TDF lasers to find a sufficient fiber cavity length for U-DSAD. The total lengths of the fiber cavities were 159 m, 262 m, 314 m, and 485 m with all-single-mode fibers. Since the material dispersion of silica glass at a wavelength of 2 μm is known as anomalous and since waveguide dispersion is not dominant in single-mode fibers with a core diameter of 8–10 μm, the total GVD of the silica fiber cavity is anomalous. The total GVD and cubic nonlinearity of the laser cavity with a 485 m long fiber cavity are -43.7 ps^2 and 0.22 W^{-1}, respectively.

Output characteristics of the mode-locked pulses generated by the low repetition rate mode-locked TDF laser with a cavity length of 159 m are shown in Fig. 7. Figure 7a shows the mode-locked pulse power profile in the time domain with a repetition rate

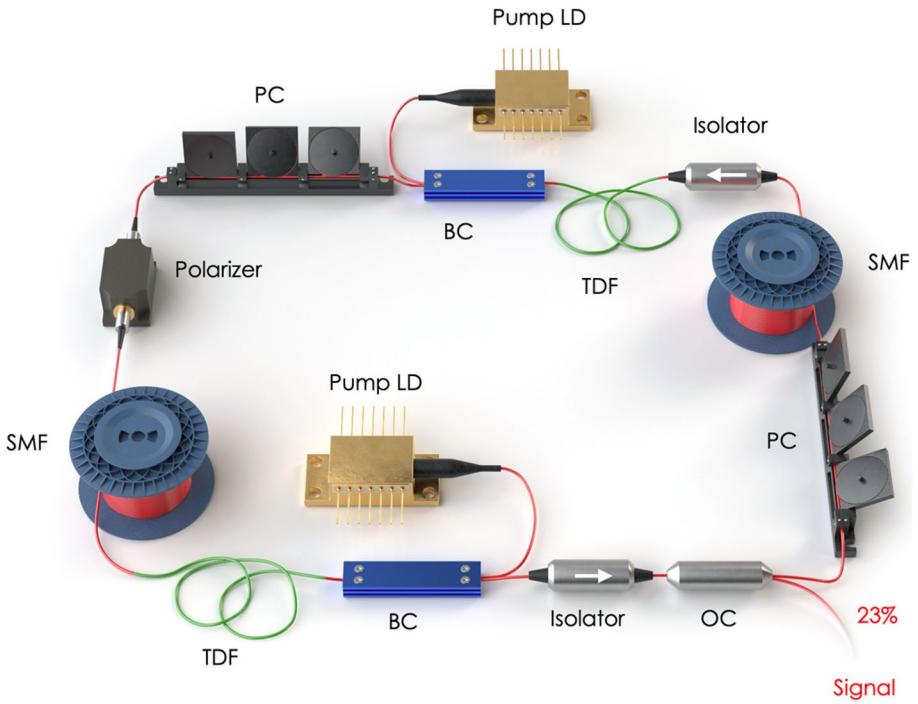

Fig. 6 Schematic of the low repetition rate mode-locked TDF laser for U-DSAD. LD: laser diode, BC: beam combiner, TDF: thulium-doped fiber, SMF: single-mode fiber, PC: polarization controller, OC: output coupler

of 1.3 MHz at 9 W pump power. As shown in Fig. 7b, the laser operation exhibits 2nd harmonic mode-locking when the pump power increases to 13 W. In U-DSAD operation, the fundamentally mode-locked pulse of the fiber laser is split into multiple pulses, and the laser operation evolves to stable harmonic mode-locking in a few seconds by the pump power increment. Figure 7c displays an intensity autocorrelation of mode-locked pulses with a 280 fs pulse duration for fundamental, 2nd harmonic, and 3rd harmonic mode-locking. Based on these results, up to now, the laser operation seems to be typical soliton mode-locking operation. But as shown in Fig. 7d, the pulse energy is significantly higher than soliton solutions. The maximum pulse energy was 20 nJ at a pump power of 11 W, where the pulse energy is evaluated directly from the average output power and repetition rate of the mode-locked pulses. To check the validity of this pulse energy evaluation, we confirmed that no continuous wave power was observed between mode-locked pulses compared to the noise signal of the detector when the input optical power was zero. The noise signal and mode-locked pulse signal are shown in the inset of Fig. 7a.

Typically, the maximum pulse energy of soliton solutions is under 10 nJ with single-mode all-fiber lasers [48–50]. In addition to this considerable difference, as shown in Fig. 8a, the obtained optical spectrum of mode-locking differs from a soliton spectrum. The shape of the spectrum is close to Gaussian rather than the hyperbolic secant function, and no Kelly sideband peak is observed. Accordingly, we presumed that the mode-locked pulses were built by dissipative resonance between anomalous dispersion and quintic nonlinearity, and we tested this conjecture with the other low repetition rate mode-locked TDF lasers with longer fiber cavity lengths. Figure 8b–d plot the optical spectra of mode-locked pulses with fiber cavity lengths of

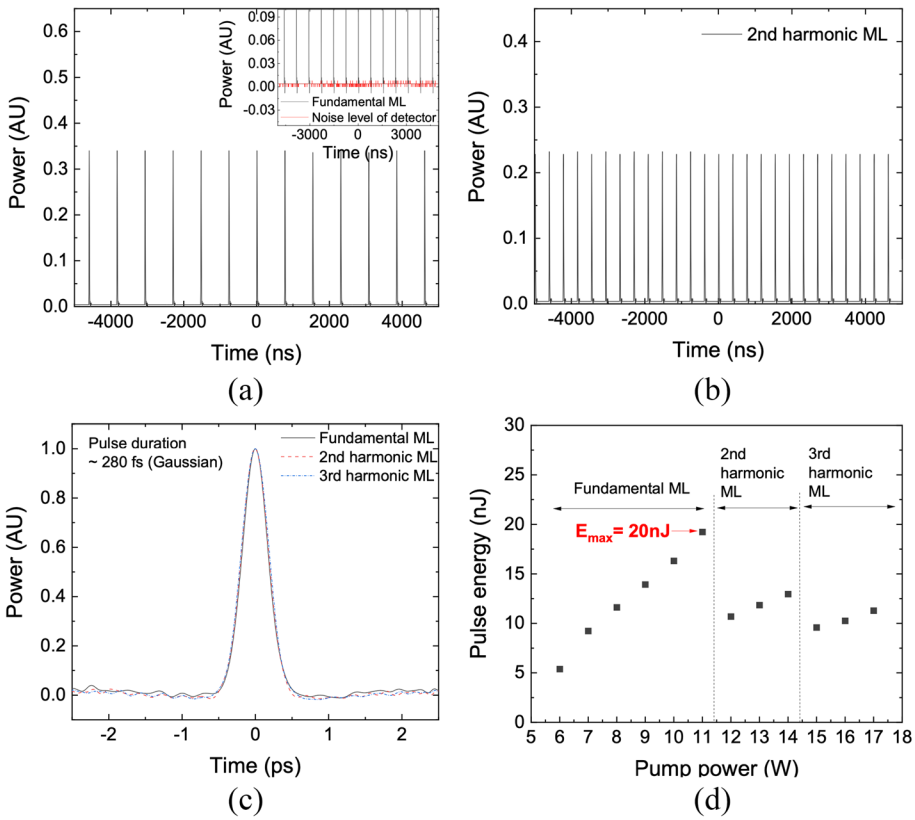

Fig. 7 Output characteristics of mode-locked pulses generated from a low repetition rate mode-locked TDF laser with a cavity length of 159 m. **a** Optical power profile of fundamental mode-locked pulses in the time domain (inset: mode-locked pulse signal compared to the noise level of the detector). **b** 2nd harmonic mode-locked pulses in the time domain. **c** Intensity autocorrelation signals for fundamental, 2nd harmonic, and 3rd harmonic mode-locked pulses. **d** Pulse energy with respect to pump power

262 m, 314 m, and 485 m, respectively. Longer fiber cavities drive the optical spectrum to have a flat-top shape. As shown in Fig. 8d, the 485 m long fiber cavity exhibits a totally flat-top spectrum with a trapezoidal shape. This kind of spectrum can typically be found in DSs in a fiber cavity with high dispersion and nonlinearity [43, 44]. It is worth noting that the flat-top spectrum cannot be achieved with fiber cavity lengths of 159 m, 262 m, or 314 m even if the pump power is increased to realize sufficient nonlinearity. We believe that a high total dispersion value of the long-length fiber cavity is crucial for the flat-top spectrum to achieve sufficient dissipative resonance without being disturbed by gain or any other components that can affect the soliton solutions. Figure 9 shows the mode-locked pulse energy with respect to pump power for the four different fiber cavity lengths. With the 159 m long fiber cavity, the maximum pulse energy was 36.1 nJ at 10 W pump power. The maximum pulse energy increased to 64 nJ with the 314 m long fiber cavity, and further increased to 80 nJ with the 485 m long fiber cavity. All of the maximum pulse energies were observed in fundamental mode-locking operation.

Figure 10 shows the characteristics of the mode-locked laser output generated from the 485 m long fiber cavity. Figure 10a and b plot the time domain intensity profile and RF spectrum, respectively, that show stable mode-locking operation at a 427 kHz

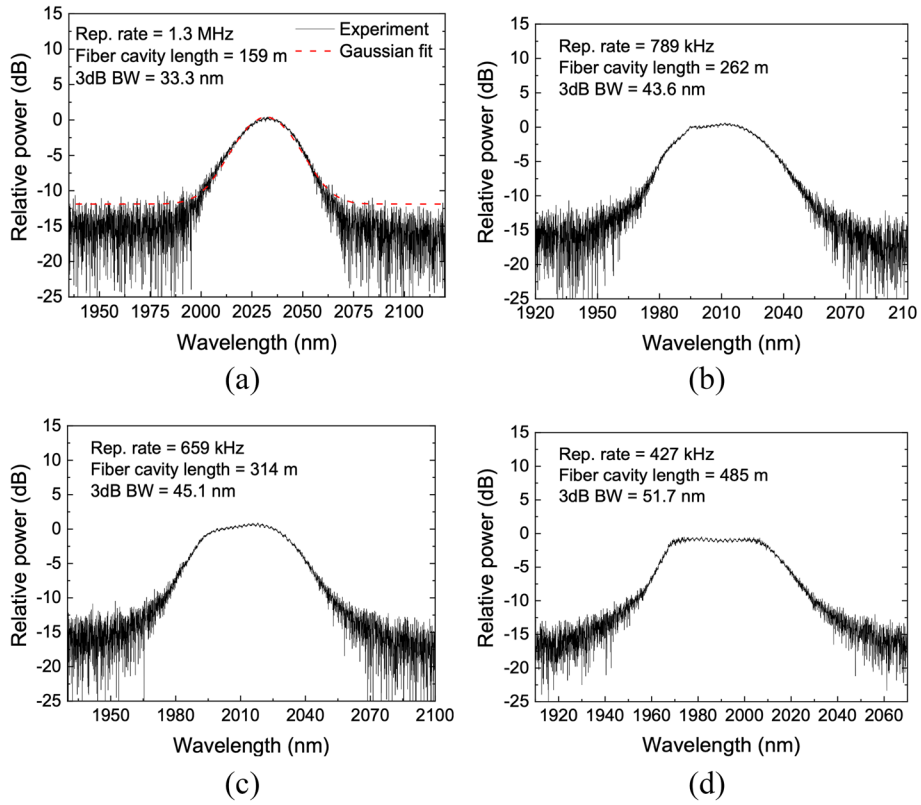

Fig. 8 Optical spectra of mode-locked pulses generated by a low repetition rate mode-locked TDF laser for U-DSAD with a fiber cavity length of (**a**) 159 m, **b** 262 m, **c** 314 m, and **d** 485 m

repetition rate. The duration of the mode-locked pulse was 249 fs assuming a Gaussian pulse shape, evaluated from the autocorrelation signal shown in Fig. 10c. At 14 W pump power, the laser operation switched to 2nd harmonic mode-locking; Fig. 10d shows the optical power profile of 2nd harmonic mode-locking in the time domain.

With this mode-locked thulium-doped fiber laser, we found that the shape of the optical spectrum depends on the pump power. Figure 10e plots the optical spectra with respect to various pump powers. The shape of the optical spectrum is mostly Gaussian at a pump power of 9 W, while at a pump power of 11 W, the spectrum shape changes to have steep edges at short wavelengths and rounded edges at long wavelengths. When the pump power is further increased to 13 W, the optical spectrum exhibits a flat-top shape. This trapezoidal shape of the optical spectrum seems to be almost identical with Fig. 2f showing the U-DSAD solution found via numerical simulation. It should be noted that the polarization states of output lasers differ by the setup for each generated result since the output laser polarization strongly depends on the birefringence of the fiber cavity and the manipulation of the polarization controller (PC) in the cavity. Nevertheless, fundamentally mode-locked pulses and harmonic mode-locked pulses generated from a laser setup are expected to have almost identical polarization states due to the fact that the PC and birefringence of the fiber are not manipulated when the pump power is increased.

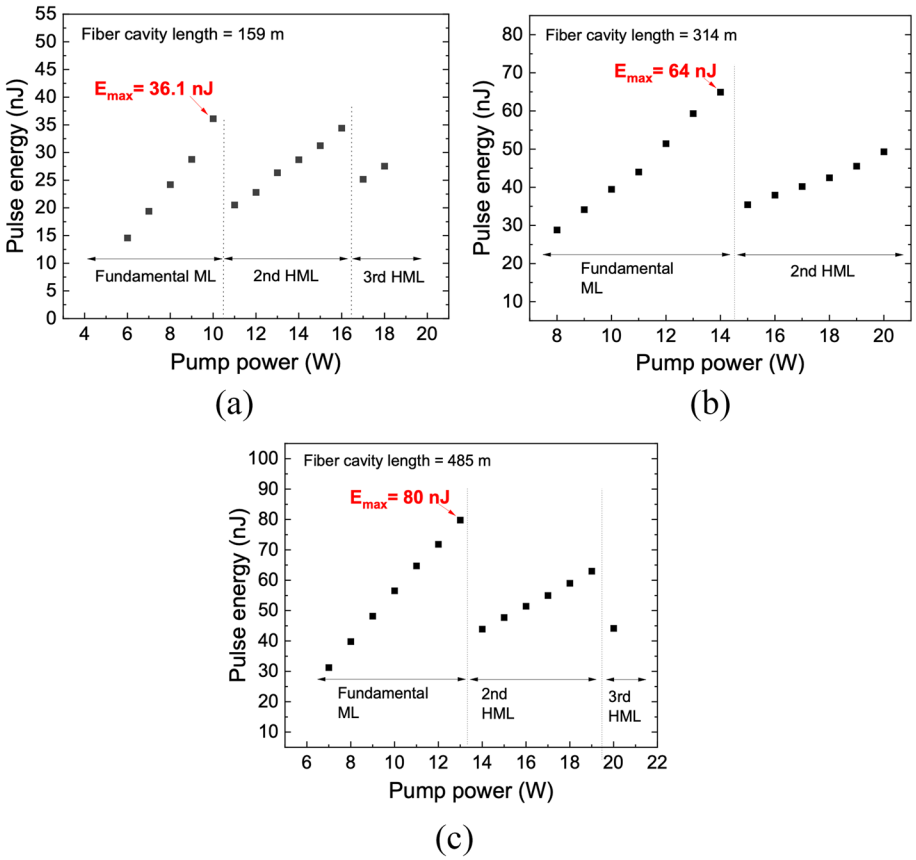

Fig. 9 Mode-locked pulse energy with respect to pump power from the low repetition rate mode-locked fiber laser with a fiber cavity length of (**a**) 159 m, **b** 314 m, and (**c**) 485 m

Based on the results of Figs. 9c and 10c, we evaluated the peak power of the mode-locked pulse to be 330 kW with the assumption that the pulse shape is Gaussian. Such a high peak power has to date not been observed in former studies on single mode-fiber lasers. We believe that dissipative resonance in anomalous dispersion led to this high peak power based on the fact that the experimental results exhibited the same four properties that were found in the numerical simulations, as follows. Matching the first property stated at the end of "Numerical calculation" section, the mode-locked pulse energy of 80 nJ found here is higher than any previously reported pulse energy of mode-locked single-mode fiber lasers. Second, as shown in Fig. 8d, the low repetition rate mode-locked thulium-doped fiber laser exhibits a flat-top optical spectrum, and moreover, the trapezoidal spectrum appears highly analogous with the optical spectrum of U-DSAD in Fig. 2f. Third, the optical spectra of the mode-locked pulses depend on the pump power. Such optical spectrum changes in anomalous dispersion are atypical, although some dispersion-managed mode-locked pulses have been shown to exhibit pump power dependence. Fourth, the present ultrafast mode-locked laser shows harmonic mode-locking. While harmonic mode-locking in anomalous dispersion is not atypical, harmonic mode-locking with a flat-top shaped spectrum is quite unusual. We also note that typical DSs

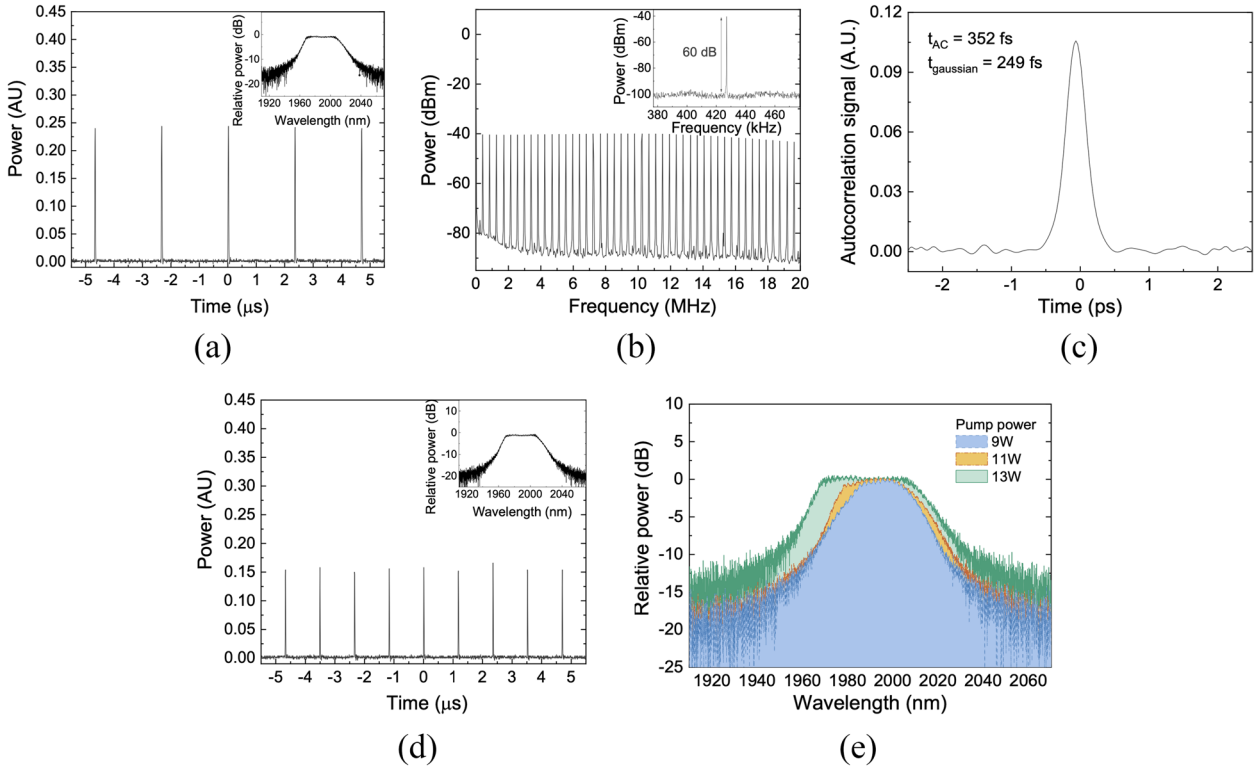

Fig. 10 Output characteristics of the low repetition rate mode-locked TDF laser with a fiber cavity length of 485 m. **a** Optical power profile of fundamental mode-locking in the time domain (inset: optical spectrum of fundamental mode-locking with a flat-top shape). **b** RF spectrum with a 20 MHz span (inset: RF peak at 427 kHz). **c** Intensity autocorrelation. **d** Optical power profile of 2nd harmonic mode-locking (inset: optical spectrum of 2nd harmonic mode-locking with a flat-top shape). **e** Pump-power-dependent optical spectra of U-DSAD

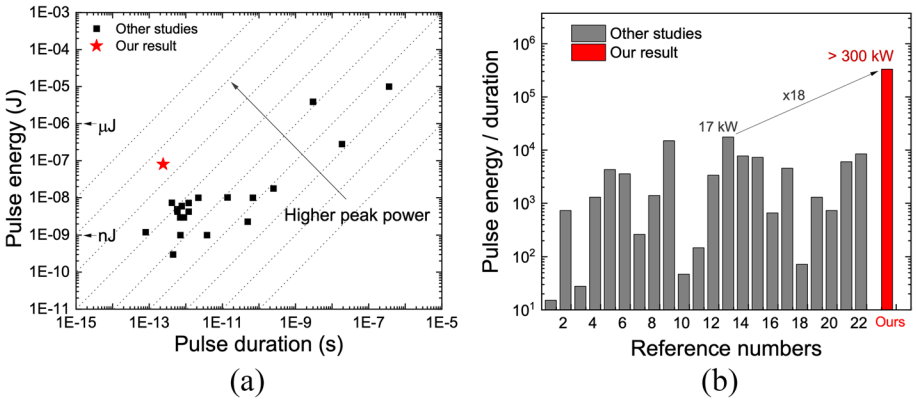

Fig. 11 **a** Pulse energy and pulse duration, and **b** roughly estimated peak power from the current study and previous studies related with high peak power or high pulse energy single-mode fiber lasers

do not exhibit harmonic mode-locking without artificial treatment, such as strong spectral filtering [51–54].

For a clear comparison of the current work with previous studies, Fig. 11a plots the pulse energy and duration referring to references related to high peak power or high pulse energy [30, 45, 47, 49, 55–71]. Based on the data in Fig. 11a, the peak power is roughly estimated and organized as in Fig. 11b. The highest peak power of mode-locked pulses among the references is about 17 kW; by comparison, our TDF laser exhibits about an 18 times higher peak power. We believe that this phenomenon is only possible by the new laser dynamics called U-DSAD.

Conclusion

We discovered and characterized the properties of U-DSAD—ultrafast dissipative solitons in a fiber cavity with anomalous group velocity dispersion—based on simulations of laser dynamics including quintic nonlinearity. Four properties of U-DSAD found in this study are distinct from typical solitons or dissipative solitons. Furthermore, the solution of U-DSAD exhibits a high peak power beyond the cubic nonlinearity limitation of typical solitons. Based on the simulation results and previous studies on DSAD in TDF lasers, we built a TDF laser that can generate mode-locked pulses having atypical properties. Their characteristics are not included in any other laser solutions but fit well into the four unique properties of U-DSAD found via simulation. The highest peak power of the laser was about 330 kW, an unprecedently high value compared to former studies on mode-locked fiber lasers with single-mode fibers. We anticipate that this first demonstration of U-DSAD will be beneficial to applications related with high peak power, such as surgical laser scalpels or nonlinear optics.

Abbreviations

GVD	Group velocity dispersion
DSAD	Dissipative solitons in anomalous GVD
TDF	Thulium-doped silica fiber
NPR	Nonlinear polarization rotation
SPM	Self-phase modulation
DS	Dissipative soliton
U-DSAD	Ultrafast dissipative solitons in a fiber cavity with anomalous group velocity dispersion
LD	Laser diode
BC	Beam combiner

Acknowledgements
Not applicable.

Authors' contributions
Jinhwa Gene and Sun Do Lim conceived the idea and initiated the project. Jinhwa Gene wrote the manuscript, produced the figures, and contributed to the simulation and experimental results. Seung Kwan Kim and Min Yong Jeon edited the manuscript. Sun Do Lim and Min Yong Jeon supervised the project. All authors read and approved the final manuscript.

Funding
This research was supported in part by the Basic Science Research Program through the National Research Foundation of Korea (NRF) funded by the Ministry of Education (NRF-2020R1A6A1A03047771), and in part by a grant from the Korea Research Institute of Standards and Science (KRISS-2023–GP2023-0002-14).

Availability of data and materials
All data needed to evaluate conclusions in the paper are present in the paper. Additional data related to this paper may be requested from the authors.

Declarations

Ethics approval and consent to participate
There is no ethics issue for this paper.

Consent for publication
All authors agreed to publish this paper.

Competing interests
The authors declare that they have no competing interests.

Received: 14 July 2023 Revised: 13 September 2023 Accepted: 27 September 2023
Published online: 16 October 2023

References

1. Shi H, et al. Review of low timing jitter mode-locked fiber lasers and applications in dual-comb absolute distance measurement. Nanotechnol Precis Eng. 2018;1:205–17.
2. Jang Y-S, Kim S-W. Distance measurements using mode-locked lasers: a review. Nanomanuf Metrol. 2018;1:131–47.
3. Vyhlídal D, Jelínek M, Čech M, Kubeček V. Performance evaluation of fast, high precision laser rangefinder electronics with a pulsed laser. Proc Spie. 2011;8306:83060D-1–7.
4. Lee J, Kim Y-J, Lee K, Lee S, Kim S-W. Time-of-flight measurement with femtosecond light pulses. Nat Photonics. 2010;4:716–20.
5. Soltanian R, Long P, Goher QS, Légaré F. All-fiber sub-20 ps ultra low repetition rate high peak power mode-locked fiber laser to generate supercontinuum. Laser Phys Lett. 2020;17:025104.
6. Alani IAM, Lokman MQ, Ahmed MHM, Al-Masoodi AHH, Latiff AA, Harun SW. A few-picosecond and high-peak-power passively mode-locked erbium-doped fibre laser based on zinc oxide polyvinyl alcohol film saturable absorber. Laser Phys. 2018;28:075105.
7. Rudy CW, Digonnet MJF, Byer RL. Advances in 2-μm Tm-doped mode-locked fiber lasers. Opt Fiber Technol. 2014;20:642–9.
8. Cai J-H, Chen S-P, Hou J. 11-kW peak-power dissipative soliton resonance in a mode-locked Yb-fiber laser. IEEE Photonics Technol Lett. 2017;29:2191–4.
9. Bale BG, Boscolo S, Kutz JN, Turitsyn SK. Intracavity dynamics in high-power mode-locked fiber lasers. Phys Rev A. 2010;81:033828.
10. Li J, et al. All-fiber passively mode-locked Tm-doped NOLM-based oscillator operating at 2-μm in both soliton and noisy-pulse regimes. Opt Express. 2014;22:7875–82.
11. Wang X, Zhou P, Wang X, Xiao H, Liu Z. Pulse bundles and passive harmonic mode-locked pulses in Tm-doped fiber laser based on nonlinear polarization rotation. Opt Express. 2014;22:6147–53.
12. Smirnov S, Kobtsev S, Kukarin S, Ivanenko A. Three key regimes of single pulse generation per round trip of all-normal-dispersion fiber lasers mode-locked with nonlinear polarization rotation. Opt Express. 2012;20:27447–53.
13. Schibli TR, Thoen ER, Kärtner FX, Ippen EP. Suppression of Q-switched mode locking and break-up into multiple pulses by inverse saturable absorption. Appl Phys B. 2000;70:S41–9.
14. Broderick NGR, Offerhaus HL, Richardson DJ, Sammut RA. Power scaling in passively mode-locked large-mode area fiber lasers. IEEE Photonics Technol Lett. 1998;10:1718–20.
15. Broderick NGR, et al. Large mode area fibers for high power applications. Opt Fiber Technol. 1999;5:185–96.
16. Liu W, et al. Single-polarization large-mode-area fiber laser mode-locked with a nonlinear amplifying loop mirror. Opt Lett. 2018;43:2848–51.
17. Ding E, Lefrancois S, Kutz JN, Wise FW. Scaling fiber lasers to large mode area: an investigation of passive mode-locking using a multi-mode fiber. IEEE J Quantum Electron. 2011;47:597–606.
18. Li C, et al. Fiber chirped pulse amplification of a short wavelength mode-locked thulium-doped fiber laser. APL Photonics. 2017;2:1213021-5i.

19. Sobon G, et al. Chirped pulse amplification of a femtosecond Er-doped fiber laser mode-locked by a graphene saturable absorber. Laser Phys Lett. 2013;10:035104.
20. Sumimura K, Yoshida H, Fujita H, Nakatsuka M. Femtosecond mode-locked Yb fiber laser for single-mode fiber chirped pulse amplification system. Laser Phys. 2007;17:339–44.
21. Stock ML, Mourou G. Chirped pulse amplification in an erbium-doped fiber oscillator/ erbium-doped fiber amplifier system. Optics Commun. 1994;106:249–52.
22. Maine P, Strickland D, Bado P, Pessot M, Mourou G. Generation of ultrahigh peak power pulses by chirped pulse amplification. IEEE J Quantum Electron. 1988;24:398–403.
23. Galvanauskas A. Mode-scalable fiber-based chirped pulse amplification systems. IEEE J Sel Top Quantum Electron. 2001;7:504–17.
24. Huttunen A, Törmä P. Optimization of dual-core and microstructure fiber geometries for dispersion compensation and large mode area. Opt Express. 2005;13:627–35.
25. Yu-lai S, Wen-tao Z, Guoling L, Yuan T, Shan T. Optimal design of large mode area all-solid-fiber using a gray relational optimization technique. Optik. 2021;242:167188.
26. Li F, et al. A large dispersion-managed monolithic all-fiber chirped pulse amplification system for high-energy femtosecond laser generation. Opt Laser Technol. 2022;147:107684.
27. Fermann ME, Sugden K, Bennion I. High-power soliton fiber laser based on pulse width control with chirped fiber Bragg gratings. Opt Lett. 1995;20:172–4.
28. Cabasse A, Martel G, Oudar JL. High power dissipative soliton in an Erbium-doped fiber laser mode-locked with a high modulation depth saturable absorber mirror. Opt Express. 2009;17:9537–42.
29. Ding E, Grelu P, Kutz JN. Dissipative soliton resonance in a passively mode-locked fiber laser. Opt Lett. 2011;36:1146–8.
30. Chongyuan H, et al. Developing high energy dissipative soliton fiber lasers at 2 micron. Sci Rep-uk. 2015;5:13680.
31 Peng J, Boscolo S, Zhao Z, Zeng H. Breathing dissipative solitons in mode-locked fiber lasers. Sci Adv. 2019;5:eaax1110.
32. Chang W, Soto-Crespo JM, Ankiewicz A, Akhmediev N. Dissipative soliton resonances in the anomalous dispersion regime. Phys Rev A. 2009;79:33840–5.
33. Liu X. Coexistence of strong and weak pulses in a fiber laser with largely anomalous dispersion. Opt Express. 2011;19:5874.
34. Duan L, Liu X, Mao D, Wang L, Wang G. Experimental observation of dissipative soliton resonance in an anomalous-dispersion fiber laser. Opt Express. 2012;20:265.
35. Zhao J, Li L, Zhao L, Tang D, Shen D. Dissipative soliton resonances in a mode-locked holmium-doped fiber laser. IEEE Photonic Tech L. 2018;30:1699–702.
36. Krzempek K, Abramski K. Dissipative soliton resonance mode-locked double clad Er: Yb laser at different values of anomalous dispersion. Opt Express. 2016;24:22379.
37. Ibarra-Escamilla B, et al. Dissipative soliton resonance in a thulium-doped all-fiber laser operating at large anomalous dispersion regime. IEEE Photonics J. 2018;10:1–7.
38. Peng J, Zeng H. Soliton collision induced explosions in a mode-locked fibre laser. Commun Phys. 2019;2:34.
39. Zhou Y, Ren Y-X, Shi J, Wong KKY. Breathing dissipative soliton explosions in a bidirectional ultrafast fiber laser. Photon Res. 2020;8:1566–72.
40. Haus HA. Theory of mode locking with a fast saturable absorber. J Appl Phys. 1975;46:3049–58.
41. Haus HA, Fellow L. Mode-locking of lasers. Sel Top Quantum Electron. 2000;6:1173–85.
42. Haus H. Parameter ranges for CW passive mode locking. IEEE J Quantum Electron. 1976;12:169–76.
43. Liu X. Dissipative soliton evolution in ultra-large normal-cavity-dispersion fiber lasers. Opt Express. 2009;17:9549.
44. Liu X. Numerical and experimental investigation of dissipative solitons in passively mode-locked fiber lasers with large net-normal-dispersion and high nonlinearity. Opt Express. 2009;17:22401–16.
45. Liu D, Zhu X, Wang C, Yu J, Hu D. Low-repetition-rate, high-energy, twin-pulse, passively mode locked Yb3+-doped fiber laser. Appl Opt. 2011;50:484–91.
46. Zhang M, Chen L, Zhou C, Cai Y, Zhang Z. Ultra-low repetition rate all-normal-dispersion linear-cavity mode-locked fiber lasers. 2009.
47. Kobtsev S, Kukarin S, Fedotov Y. Ultra-low repetition rate mode-locked fiber laser with high-energy pulses. Opt Express. 2008;16:21936–41.
48. Liu XM, Mao D. Compact all-fiber high-energy fiber laser with sub-300-fs duration. Opt Express. 2010;18:8847–52.
49. Jeong H, et al. All-fiber Tm-doped soliton laser oscillator with 6 nJ pulse energy based on evanescent field interaction with monoloayer graphene saturable absorber. Opt Express. 2016;24:14152.
50. Choi SY, Jeong H, Hong BH, Rotermund F, Yeom D-I. All-fiber dissipative soliton laser with 10.2 nJ pulse energy using an evanescent field interaction with graphene saturable absorber. Laser Phys Lett. 2014;11:15101.
51. Zhu X, Wang C, Liu S, Zhang G. Tunable high-order harmonic mode-locking in Yb-doped fiber laser with all-normal dispersion. IEEE Photonics Technology Letters. 2012;24:754–6.
52. Wang J, et al. All-normal-dispersion passive harmonic mode-locking 220 fs ytterbium fiber laser. Appl Optics. 2014;53:5088.
53. Peng J, Zhan L, Luo S, Shen Q. Passive harmonic mode-locking of dissipative solitons in a normal-dispersion Er-doped fiber laser. J Lightwave Technol. 2013;31:3009–14.
54. Huang SS, et al. High order harmonic mode-locking in an all-normal-dispersion Yb-doped fiber laser with a graphene oxide saturable absorber. Laser Phys. 2013;24:015001.
55. Wu X, Tang DY, Zhang H, Zhao LM. Dissipative soliton resonance in an all-normaldispersion erbium-doped fiber laser. Opt Express. 2009;17:5580.
56. Choi SY, Jeong H, Hong BH, Rotermund F, Yeom D-I. All-fiber dissipative soliton laser with 10.2 nJ pulse energy using an evanescent field interaction with graphene saturable absorber. Laser Phys Lett. 2013;11:015101.
57. Semaan G, et al. 10 μJ dissipative soliton resonance square pulse in a dual amplifier figure-of-eight double-clad Er: Yb mode-locked fiber laser. Opt Lett. 2016;41:4767.

58. Zhang H, Bao Q, Tang D, Zhao L, Loh K. Large energy soliton erbium-doped fiber laser with a graphene-polymer composite mode locker. Appl Phys Lett. 2009;95:141103.
59. Engelbrecht M, Haxsen F, Ruehl A, Wandt D, Kracht D. Ultrafast thulium-doped fiber-oscillator with pulse energy of 4.3 nJ. Opt Lett. 2008;33:690–2.
60. Sayinc H, Mortag D, Wandt D, Neumann J, Kracht D. Sub-100 fs pulses from a low repetition rate Yb-doped fiber laser. Opt Express. 2009;17:5731–5.
61. Chen T, Liao C, Wang DN, Wang Y. Passively mode-locked fiber laser by using monolayer chemical vapor deposition of graphene on D-shaped fiber. Appl Opt. 2014;53:2828–32.
62. Chong A, Renninger WH, Wise FW. Route to the minimum pulse duration in normal-dispersion fiber lasers. Opt Lett. 2008;33:2638–40.
63. Zhang H, et al. Graphene mode locked, wavelength-tunable, dissipative soliton fiber laser. Appl Phys Lett. 2010;96:111112.
64. Rodriguez-Morales LA, et al. Long cavity ring fiber mode-locked laser with decreased net value of nonlinear polarization rotation. Opt Express. 2019;27:14030–40.
65. Chamorovskiy A, et al. Femtosecond mode-locked holmium fiber laser pumped by semiconductor disk laser. Opt Lett. 2012;37:1448–50.
66. Zhang H, Tang DY, Zhao LM, Bao QL, Loh KP. Large energy mode locking of an erbium-doped fiber laser with atomic layer graphene. Opt Express. 2009;17:17630–5.
67. Jung M, et al. Mode-locked pulse generation from an all-fiberized, Tm-Ho-codoped fiber laser incorporating a graphene oxide-deposited side-polished fiber. Opt Express. 2013;21:20062–72.
68. Kadel R, Washburn BR. Stretched-pulse and solitonic operation of an all-fiber thulium/holmium-doped fiber laser. Appl Opt. 2015;54:746–50.
69. Wan P, Yang L-M, Liu J. High pulse energy 2 μm femtosecond fiber laser. Opt Express. 2013;21:1798–803.
70. Song Y-W, Jang S-Y, Han W-S, Bae M-K. Graphene mode-lockers for fiber lasers functioned with evanescent field interaction. Appl Phys Lett. 2010;96:051122.
71. Junting L, et al. High output mode-locked laser empowered by defect regulation in 2D Bi2O2Se saturable absorber. Nat Commun. 2022;13:3855.

Publisher's Note